

The quantum walker probes her coin parameter

Shivani Singh* and C. M. Chandrashekar†

The Institute of Mathematical Sciences, C. I. T, campus, Taramani, Chennai, 600113, India and Homi Bhabha National Institute, Training School Complex, Anushakti Nagar, Mumbai 400094, India

Matteo G. A. Paris‡

Quantum Technology Lab, Dipartimento di Fisica Aldo Pontremoli, Università degli Studi di Milano, I-20133 Milano, Italia

In discrete-time quantum walk (DTQW) the walkers coin space entangles with the position space after the very first step of the evolution. This phenomenon may be exploited to obtain the value of the coin parameter θ by performing measurements on the sole position space of the walker. In this paper, we evaluate the ultimate quantum limits to precision for this class of estimation protocols, and use this result to assess measurement schemes having limited access to the position space of the walker. We find that the quantum Fisher information (QFI) of the walker's position space $H_w(\theta)$ increases with θ and with time which, in turn, may be seen as a metrological resource. We also find a difference in the QFI of *bounded* and *unbounded* DTQWs, and provide an interpretation of the different behaviours in terms of interference in the position space. Finally, we compare $H_w(\theta)$ to the full QFI $H_f(\theta)$, i.e. the QFI of the walkers position + coin state, and find that their ratio is dependent on θ , but saturates to a constant value, meaning that the walker may probe its coin parameter quite faithfully.

I. INTRODUCTION

Quantum walk is the quantum analogue of random walk which, in turn, provides a relevant model for the dynamics of various classical systems [1, 2]. Quantum superposition and interference strongly affects the dynamics of a quantum walker and this leads to a quadratically faster spread in position space when compared to a classical walker [3–9]. This feature made quantum walks a powerful tool in quantum computation [10–14], as well as to model the dynamics of different quantum systems, such as energy transport in photosynthesis [15, 16], quantum percolation [17, 18], and graph isomorphism [19].

As in classical random walk, quantum walks has also been developed in two forms, continuous-time (CTQW) and discrete-time quantum walk (DTQW). Both the variants have been shown to efficiently implement any quantum computational tasks [19, 20]. Continuous-time quantum walk is defined only on position Hilbert space whereas, discrete-time quantum walk is defined on a joint position and *coin* Hilbert space, thus providing additional degree of freedom to control the dynamics. Upon tuning the different parameters of the evolution operators of DTQW, one may control and engineer the dynamics in order to *simulate* various quantum phenomena such as localization [21–23], topological phase [24, 25], neutrino oscillation [26, 27] and relativistic quantum dynamics [28–34]. Quantum walks have been experimentally implemented in various physical systems such as NMR [35], photonic [36–39], cold atoms [40] and trapped ions [41, 42].

Evolution in discrete-time quantum walk is defined by unitary *coin operation* followed by a unitary *position shift operator*. Shift operator evolves the walker in a superposition of the position states, with amplitudes governed by the operation on coin Hilbert space. The most general unitary coin operator has four independent parameters [43] and provides an ample control over the dynamics, but already one- and two-parameter coins are extremely useful in simulating various physical systems. For example, different combination of evolution parameter in split-step DTQW describes topological phases [24, 25] and neutrino oscillation [26, 27]. Indeed, coin parameters play a relevant role in the evolution of the state of the walker in the position space and, in turn, in controlling and engineering DTQWs. In this framework, a precise knowledge of the coin parameters is a crucial information for quantum simulations and for further development in the use of quantum walks to model realistic quantum dynamics.

In this paper, we consider a coin operator with one parameter θ and address the evolution of bounded and unbounded DTQWs. Our aim is to design optimal estimation techniques for the coin parameter based on measurements performed on the sole position space of the walker. Our approach belongs to the class of protocols usually referred to as quantum probing [44–55], which proved useful to precisely extract information upon exploiting the inherent sensitivity of quantum systems to external perturbations.

We use the Fisher information (FI) to quantify the information about a parameter θ which may be extracted by performing a given measurement on a quantum system. In particular, we consider the FI $F_w(\theta)$ of the generic measurement performed on the walker's position degree of freedom. The maximum of $F_w(\theta)$ over all the possible measurements is the so-called quantum Fisher information $H_w(\theta)$ (QFI), which quantifies the ultimate

* shivanis@imsc.res.in

† chandru@imsc.res.in

‡ matteo.paris@fisica.unimi.it

quantum bound to the extractable information, i.e. the overall information encoded onto the state of the system. We also evaluate the full QFI $H_f(\theta)$, i.e. the QFI of the position+coin state, in order to assess the overall performances of measurements on the sole position space of the walker, compared to measurements having access to the full quantum state. Our results show that the walker QFI $H_w(\theta)$ increases as t^2 , as it happens for the full QFI $H_f(\theta)$, meaning that the walker is a good probe for its coin operation parameter θ . Besides, the walker's position QFI $H_w(\theta)$ increases with θ and then decreases slowly upto $\pi/2$ (and then mimics in the mirrored way, due to symmetry in the coin operator upto π). Finally, we analyze in some detail the performances of position measurement on the walker, i.e. we assess how much information on the coin parameter may be extracted by looking at the probability distribution of the walker at a given time.

The paper is structured as follows. In Section II, we describe bounded and unbounded DTQWs and the evolution operators governing their dynamics. In Section III we review quantum estimation theory, describe a method to numerically calculate the walker's quantum Fisher information in DTQWs, and illustrate the main results of our analysis. Section IV closes the paper with some concluding remarks.

II. EVOLUTION IN DISCRETE-TIME QUANTUM WALK

DTQW of a single walker on a one dimensional lattice is defined on the Hilbert space $\mathcal{H} = \mathcal{H}_c \otimes \mathcal{H}_p$ where \mathcal{H}_p and \mathcal{H}_c are the position and the coin Hilbert spaces of the walker, respectively. The basis state of the coin Hilbert space are $\{|\uparrow\rangle, |\downarrow\rangle\}$ which may be seen as the internal states of the walker. The position Hilbert space is spanned by the basis $|x\rangle$ where $x \in \mathbb{Z}$. The initial state of the system is usually taken of the form

$$|\Psi_{\text{in}}\rangle = \alpha |\uparrow\rangle + \beta |\downarrow\rangle \otimes |x=0\rangle \quad ; \quad |\alpha|^2 + |\beta|^2 = 1. \quad (1)$$

Here α and β are the amplitudes of the states $|\uparrow\rangle$ and $|\downarrow\rangle$, respectively. The evolution operator for discrete-time quantum walk is defined by the action of unitary quantum coin operation followed by a position shift operator. The single parameter coin operator is given by,

$$C_\theta = \begin{pmatrix} \cos \theta & -i \sin \theta \\ -i \sin \theta & \cos \theta \end{pmatrix} \otimes \sum_x |x\rangle \langle x| \quad (2)$$

whereas the shift operator S is defined with reference to the size of the region accessible by the walker. *Unbounded* DTQWs are defined on a position Hilbert space of infinite size. The walker have no boundary condition on probability amplitude and the position shift operator is given by

$$S_x = \sum_x |\uparrow\rangle \langle \uparrow| \otimes |x-1\rangle \langle x| + |\downarrow\rangle \langle \downarrow| \otimes |x+1\rangle \langle x|. \quad (3)$$

In Fig. 1 we show the probability distribution after 200-time steps for an unbounded DTQW using different values of coin parameter θ . The smaller is the value of θ , the larger is the spread of the probability distribution. *Bounded* DTQWs evolve instead on finite position Hilbert spaces, characterized by a finite number of sites and boundary conditions. In turn, the position shift operator is bounded between $[-a, a]$ with boundary condition $|\Psi_{a+1}\rangle = |\Psi_{-a-1}\rangle = 0$, where $a \in \mathbb{Z}$. In formula,

$$S_x = |\downarrow\rangle \langle \uparrow| \otimes |-a\rangle \langle -a| + \sum_{x=-a+1}^a |\uparrow\rangle \langle \uparrow| \otimes |x-1\rangle \langle x| + \sum_{x=-a}^{a-1} |\downarrow\rangle \langle \downarrow| \otimes |x+1\rangle \langle x| + |\uparrow\rangle \langle \downarrow| \otimes |a\rangle \langle a|. \quad (4)$$

The insets of Fig. 1 show the probability distribution after 200-time step for a bounded DTQW and for different values of θ . The position space is bounded between $[-50, 50]$. In this case the shape of the probability distribution arises from the interplay of the coin operator and the bounded nature of the position space, and the spread cannot be simply characterised as function of θ , as it was for unbounded walk.

In general, after t - steps in the evolution, the overall state of the particle will be of the form,

$$|\Psi_t\rangle = \left(S_x C_\theta \right)^t |\Psi_{\text{in}}\rangle = \sum_x \left(\mathcal{A}_{x,t} |\uparrow\rangle + \mathcal{B}_{x,t} |\downarrow\rangle \right) \quad (5)$$

where $\mathcal{A}_{x,t}$ and $\mathcal{B}_{x,t}$ are the amplitudes of the state $|\uparrow\rangle$ and $|\downarrow\rangle$ at position x at time t , respectively. The \mathcal{A}, \mathcal{B} coefficients are in turn linked by the iterative relations

$$\begin{pmatrix} \mathcal{A}_{x,t} \\ \mathcal{B}_{x,t} \end{pmatrix} = \begin{pmatrix} \cos \theta & -i \sin \theta \\ 0 & 0 \end{pmatrix} \begin{pmatrix} \mathcal{A}_{x+1,t-1} \\ \mathcal{B}_{x+1,t-1} \end{pmatrix} + \begin{pmatrix} 0 & 0 \\ -i \sin \theta & \cos \theta \end{pmatrix} \begin{pmatrix} \mathcal{A}_{x-1,t-1} \\ \mathcal{B}_{x-1,t-1} \end{pmatrix} \quad (6)$$

for both, unbounded and bounded discrete-time quantum walk (when the walker is away from the boundary). Therefore, the probability of finding the particle at position x and at time t is given by,

$$P(x, t) = |\mathcal{A}_{x,t}|^2 + |\mathcal{B}_{x,t}|^2. \quad (7)$$

III. QUANTUM ESTIMATION IN DISCRETE-TIME QUANTUM WALK

The Fisher information provides a measure of the amount of information that the observable X carries about a parameter ξ , usually a quantity of interest, influencing its probability distribution $p(x|\xi)$ [56]. More in details, the Fisher information $FI(\xi)$ of a conditional distribution $p(x|\xi)$ is given by,

$$FI(\xi) = \int dx p(x|\xi) \left[\frac{\partial \log p(x|\xi)}{\partial \xi} \right]^2, \quad (8)$$

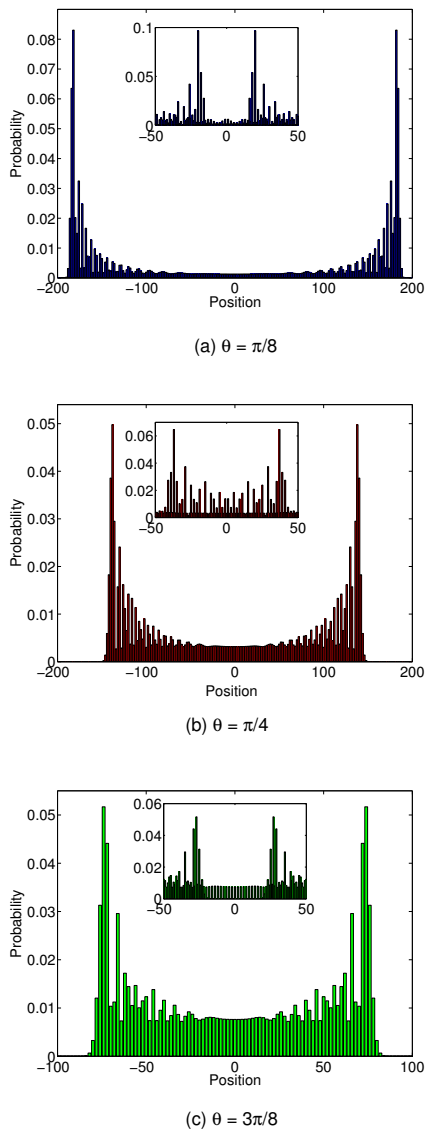


FIG. 1. Probability distribution of unbounded DTQW in one dimension after 200 time steps for different values of θ . The insets show the corresponding distributions for a DTQW bounded in the region $[-50, 50]$. In both cases the initial state of the system has been set to $\frac{1}{\sqrt{2}}(|\uparrow\rangle + |\downarrow\rangle) \otimes |x=0\rangle \equiv |+\rangle \otimes |0\rangle$.

where, as mentioned above, $p(x|\xi)$ is the probability of obtaining the outcome x from the measurement of X when the true value of parameter is ξ . If the available data for the observable X are coming from M repeated independent measurements of X , i.e. $\mathbf{x} = (x_1, x_2, \dots, x_M)$, then the overall probability of the sample (the likelihood) is $p(\mathbf{x}|\xi) = \prod_{k=1}^M p(x_k|\xi)$ which depends upon the parameter ξ to be estimated. An *estimator* $\hat{\xi}(\mathbf{x})$ is a function of the data sample, which provides an estimate of the value of the parameter ξ . Since data fluctuate, the value of the estimator fluctuates as well. The variance $\text{Var}_{\xi}\hat{\xi}$ of $\hat{\xi}$ provides a measure of the pre-

cision of the overall estimation procedure (i.e. the measurement of X followed by the data processing $\hat{\xi}$). The Cramer-Rao theorem states that the Fisher information poses a bound of the variance of $\hat{\xi}$

$$\text{Var}_{\xi}\hat{\xi} \geq \frac{1}{MF(\xi)}. \quad (9)$$

The larger is $F(\xi)$ the larger is the information about ξ that *may* be, *in principle* extracted from the measurement of X . The actual information on ξ obtained from measuring X does instead depend on the estimator. An estimator saturating the Cramer-Rao bound of Eq. (9) is said to be *efficient*. In the following, we assume that an efficient estimator is available and compare the performances of different measurements in terms of their Fisher information.

Let us now move to quantum measurements: According to the Born's rule the conditional distribution $p(x|\xi)$ may be written as $p(x|\xi) = \text{Tr}[\Pi_x \rho_{\xi}]$ where, Π_x is the probability operator-valued measure (POVM) of the measured quantity X , and the dependence on ξ is encoded onto the preparation of the system undergoing the measurement, i.e the density ρ_{ξ} . An upper-bound on the Fisher information of *any* quantum measurement may be obtained by introducing the Symmetric Logarithmic Derivative (SLD) L_{ξ} , which satisfies the relation

$$\frac{1}{2} (L_{\xi}\rho_{\xi} + \rho_{\xi}L_{\xi}) = \frac{\partial\rho_{\xi}}{\partial\xi}. \quad (10)$$

Then, since $\partial_{\xi}p(x|\xi) = \text{Tr}[\partial_{\xi}\rho_{\xi}\Pi_x] = \text{Re}(\text{Tr}[\rho_{\xi}\Pi_x L_{\xi}])$, the Fisher information may be rewritten in terms of L_{ξ} and an upper-bound on Fisher information, usually referred to as *Quantum Fisher Information* (QFI), may be found

$$F(\xi) \leq H(\xi) \equiv \text{Tr}[\rho_{\xi} L_{\xi}^2] \quad (11)$$

where L_{ξ} is given in Eq. (10). For pure state, $\rho_{\xi}^2 = \rho_{\xi}$ and therefore $\partial_{\xi}\rho_{\xi} = (\partial_{\xi}\rho_{\xi})\rho_{\xi} + \rho_{\xi}(\partial_{\xi}\rho_{\xi})$ implies, $L_{\xi} = 2\partial_{\xi}\rho_{\xi}$. Hence, encoding $\rho_{\xi} = |\psi_{\xi}\rangle\langle\psi_{\xi}|$, the SLD reduces to $L_{\xi} = 2\partial_{\xi}\rho_{\xi}$.

A. The full QFI $H_f(\theta)$ in discrete-time quantum walk

The density matrix of the full (coin + position) state in the complete Hilbert space $\mathcal{H} = \mathcal{H}_c \otimes \mathcal{H}_w$ at time t is given by,

$$\rho_{\theta} = |\Psi_{\theta}\rangle\langle\Psi_{\theta}| \equiv \begin{pmatrix} |\psi_{\theta}^{\uparrow}\rangle \\ |\psi_{\theta}^{\downarrow}\rangle \end{pmatrix} \begin{pmatrix} \langle\psi_{\theta}^{\uparrow}| \\ \langle\psi_{\theta}^{\downarrow}| \end{pmatrix}^T \quad (12)$$

where the size of the vector $|\psi_{\theta}^{\uparrow}\rangle$ and $|\psi_{\theta}^{\downarrow}\rangle$ is equal to the dimension of the walker's position Hilbert space \mathcal{H}_w and

the dimension of ρ_θ is $2N$ where N is the dimension of \mathcal{H}_w . This implies that $\partial_\theta \rho_\theta$ may be written as

$$\begin{aligned} \partial_\theta \rho_\theta &= |\partial_\theta \Psi_\theta\rangle \langle \Psi_\theta| + |\Psi_\theta\rangle \langle \partial_\theta \Psi_\theta| \\ &= \begin{pmatrix} |\partial_\theta \psi_\theta^\uparrow\rangle \\ |\partial_\theta \psi_\theta^\downarrow\rangle \end{pmatrix} \begin{pmatrix} \langle \psi_\theta^\uparrow| \\ \langle \psi_\theta^\downarrow| \end{pmatrix}^T + \begin{pmatrix} |\psi_\theta^\uparrow\rangle \\ |\psi_\theta^\downarrow\rangle \end{pmatrix} \begin{pmatrix} \langle \partial_\theta \psi_\theta^\uparrow| \\ \langle \partial_\theta \psi_\theta^\downarrow| \end{pmatrix}^T \end{aligned} \quad (13)$$

and $|\partial_\theta \Psi_\theta\rangle$ at time t is given by,

$$|\partial_\theta \Psi_\theta(t)\rangle = S_x C_\theta |\partial_\theta \Psi_\theta(t-1)\rangle + S_x (\partial_\theta C_\theta) |\Psi_\theta(t-1)\rangle \quad (14)$$

where, $\partial_\theta C_\theta$ is,

$$\partial_\theta C_\theta = \begin{pmatrix} -\sin \theta & -i \cos \theta \\ -i \cos \theta & -\sin \theta \end{pmatrix} \otimes \sum_x |x\rangle \langle x|. \quad (15)$$

As a consequence, if at a given time t , we have the amplitude $\Psi_x = (\psi_x^\uparrow; \psi_x^\downarrow) = (\mathcal{A}_x, \mathcal{B}_x)$, then the iterative form for $|\partial_\theta \Psi_\theta(t)\rangle$ is given by,

$$\begin{aligned} \begin{pmatrix} \partial_\theta \mathcal{A}_{t,x} \\ \partial_\theta \mathcal{B}_{t,x} \end{pmatrix} &= \begin{pmatrix} \cos(\theta) & -i \sin(\theta) \\ 0 & 0 \end{pmatrix} \begin{pmatrix} \partial_\theta \mathcal{A}_{t-1,x+1} \\ \partial_\theta \mathcal{B}_{t-1,x+1} \end{pmatrix} \\ &+ \begin{pmatrix} 0 & 0 \\ -i \sin \theta & \cos \theta \end{pmatrix} \begin{pmatrix} \partial_\theta \mathcal{A}_{t-1,x-1} \\ \partial_\theta \mathcal{B}_{t-1,x-1} \end{pmatrix} \\ &+ \begin{pmatrix} -\sin \theta & -i \cos \theta \\ 0 & 0 \end{pmatrix} \begin{pmatrix} \mathcal{A}_{t-1,x+1} \\ \mathcal{B}_{t-1,x+1} \end{pmatrix} \\ &+ \begin{pmatrix} 0 & 0 \\ -i \cos \theta & -\sin \theta \end{pmatrix} \begin{pmatrix} \mathcal{A}_{t-1,x-1} \\ \mathcal{B}_{t-1,x-1} \end{pmatrix}. \end{aligned} \quad (16)$$

Upon substituting Eqs. (12) and (13) in Eq. (11) we obtain the quantum Fisher information $H_f(\theta)$ in the complete Hilbert space $\mathcal{H} = \mathcal{H}_c \otimes \mathcal{H}_w$, i.e. the information extractable from the full quantum state of the walker's position + coin system. In Fig. 2 we show $H_f(\theta)$ for unbounded and bounded DTQW after 200-time steps. The full QFI $H_f(\theta)$ increases as t^2 with time and it is the same for bounded and unbounded DTQWs.

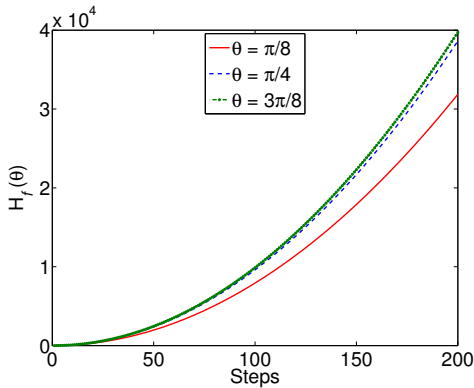


FIG. 2. The full QFI $H_f(\theta)$ as a function of time for different values of θ . The initial state of the system is $|+\rangle \otimes |0\rangle$. The full QFI $H_f(\theta)$ is the same for bounded and unbounded DTQWs.

B. The walker's position space QFI $H_w(\theta)$ in discrete-time quantum walk

The density matrix of the sole position space of the walker is obtained by tracing out the coin degree of freedom from Eq. (12). We have

$$\rho_w(\theta) = |\psi_\theta^\uparrow\rangle \langle \psi_\theta^\uparrow| + |\psi_\theta^\downarrow\rangle \langle \psi_\theta^\downarrow|, \quad (17)$$

and, in turn,

$$\begin{aligned} \partial_\theta \rho_w(\theta) &= |\partial_\theta \psi_\theta^\uparrow\rangle \langle \psi_\theta^\uparrow| + |\psi_\theta^\uparrow\rangle \langle \partial_\theta \psi_\theta^\uparrow| \\ &+ |\partial_\theta \psi_\theta^\downarrow\rangle \langle \psi_\theta^\downarrow| + |\psi_\theta^\downarrow\rangle \langle \partial_\theta \psi_\theta^\downarrow| \end{aligned} \quad (18)$$

which is equal to tracing out the coin from the derivative of the full density matrix in complete Hilbert space, i.e. tracing out the coin from Eq. (13),

$$\partial_\theta \rho_w(\theta) = \text{Tr}_c \left[\partial_\theta \rho_\theta \right]. \quad (19)$$

Density matrix in position space will be in mixed state. In mixed state, $\rho_\theta^2 = \rho_\theta + \rho_1(\theta)$ with $\rho_1(\theta) = \frac{\epsilon}{2} \int d\theta (\lambda \rho_\theta + \rho_\theta \lambda) + O(\epsilon^2)$ where $\epsilon \rightarrow 0$ and therefore SLD is $L_\theta = 2\partial_\theta \rho_\theta + \epsilon \lambda$. This implies that,

$$\begin{aligned} L^2 &= 4(\partial_\theta \rho_\theta)^2 + 2\epsilon \left[\lambda \partial_\theta \rho_\theta + (\partial_\theta \rho_\theta) \lambda \right] + O(\epsilon^2) \\ L^2 &\approx 4(\partial_\theta \rho_\theta)^2 + 2 \left[(L - 2\partial_\theta \rho_\theta) \partial_\theta \rho_\theta + \partial_\theta \rho_\theta (L - 2\partial_\theta \rho_\theta) \right] \\ L^2 &\approx -4(\partial_\theta \rho_\theta)^2 + 2(\partial_\theta \rho_\theta L + L \partial_\theta \rho_\theta) \end{aligned} \quad (20)$$

and therefore quantum Fisher information in mixed state can be given by,

$$\begin{aligned} H_w &= \text{Tr}[\rho_\theta L^2] \\ &\approx -4\text{Tr}[\rho_\theta (\partial_\theta \rho_\theta)^2] + 2\text{Tr}[\rho_\theta (\partial_\theta \rho_\theta L + L \partial_\theta \rho_\theta)] \\ &= 2\text{Tr}[\partial_\theta \rho_\theta (L \rho_\theta + \rho_\theta L)] - 4\text{Tr}[\rho_\theta (\partial_\theta \rho_\theta)^2] \\ &= 4\text{Tr} \left[(\partial_\theta \rho_\theta)^2 (\mathbb{I} - \rho_\theta) \right] \end{aligned} \quad (21)$$

This expression for quantum Fisher information for mixed state is obtained with an approximation that the higher power of ϵ are very small and thus ignoring them. Also as the time increases the size of the position space with non-zero probability also increases and purity of the states stabilises after first few steps (< 10) of the DTQW.

Fig. 3 illustrates the behaviour of $H_w(\theta)$ as a function of time for different values of θ and for both bounded and unbounded DTQW. As we have seen for the full QFI $H_f(\theta)$, also $H_w(\theta)$ increases as t^2 . For t large enough (say $t > 10$), we have $H_w(\theta) = \kappa t^2$, with the constant depending only on θ , $\kappa \equiv \kappa(\theta)$. However, some striking differences between the two cases appear after $2a$ time steps, $[-a, a]$ being the spatial interval for bounded DTQW. Those differences may be traced back to interference [57] and recurrence [58, 59] in the position space. In order to illustrate this phenomenon, in Fig. 4 we show the time

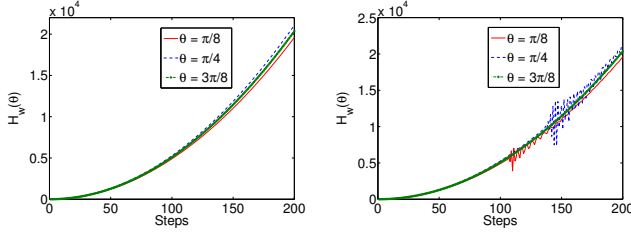


FIG. 3. The walker's position space QFI $H_w(\theta)$ as a function of time for different values of θ . Due to interference effects, we see clear differences between the walker's position space QFIs of bounded and unbounded DTQWs. The initial state of the system in both cases is $|+\rangle \otimes |0\rangle$.

evolution of the so-called *degree of interference* in the position Hilbert space. That is given by the quantity

$$\begin{aligned} \mu_{x,t+1} = & \left| \sin \theta \cos \theta \left[\rho_{p,t}^{\uparrow\downarrow}(x+1) \right. \right. \\ & \left. \left. - \rho_{p,t}^{\uparrow\downarrow}(x-1) \right] \right. \\ & \left. + \sin \theta \cos \theta \left[\rho_{p,t}^{\downarrow\uparrow}(x+1) \right. \right. \\ & \left. \left. - \rho_{p,t}^{\downarrow\uparrow}(x-1) \right] \right|, \end{aligned} \quad (22)$$

defined for any site x at the time $t+1$ which is the interference term in the evolution of the probability amplitude. At any site x at time t in the form of probability is given by,

$$\begin{aligned} P_{x,t+1} = & \cos^2 \theta \left(\rho_t^{\uparrow\uparrow}(x+1) + \rho_t^{\downarrow\downarrow}(x-1) \right) \\ & + \sin^2 \theta \left(\rho_t^{\uparrow\uparrow}(x-1) + \rho_t^{\downarrow\downarrow}(x+1) \right) \\ & + \sin \theta \cos \theta \left(\rho_t^{\uparrow\downarrow}(x+1) - \rho_t^{\uparrow\downarrow}(x-1) \right) \\ & + \sin \theta \cos \theta \left(\rho_t^{\downarrow\uparrow}(x+1) - \rho_t^{\downarrow\uparrow}(x-1) \right). \end{aligned} \quad (23)$$

As it is apparent by comparing Figs. 3 and 4, the difference between $H_w(\theta)$ of bounded and unbounded DTQW starts to appear in correspondence of the time step for which also the degree of interference of the two cases starts to differ, since the interference at a position x at time t in bounded walk is not only due to the neighbouring sites but it is due to the multiple sites. As for example, in Fig. 4-(b), it can be seen that for $\theta = \pi/8$, the degree of interference initially spreads over the position space with time, and then starts to come back at the initial position state. After $t = 100$ time steps, interference between the reflected waves dominates, as we have seen for the QFI $H_w(\theta)$. A similar behaviour (see Fig. 3 and the other panels of Fig. 4) may be observed for the other values of θ .

Fig. 5 shows the ratio, $H_w(\theta)/H_f(\theta)$ between the QFI of the walker's position space and the full QFI. As it

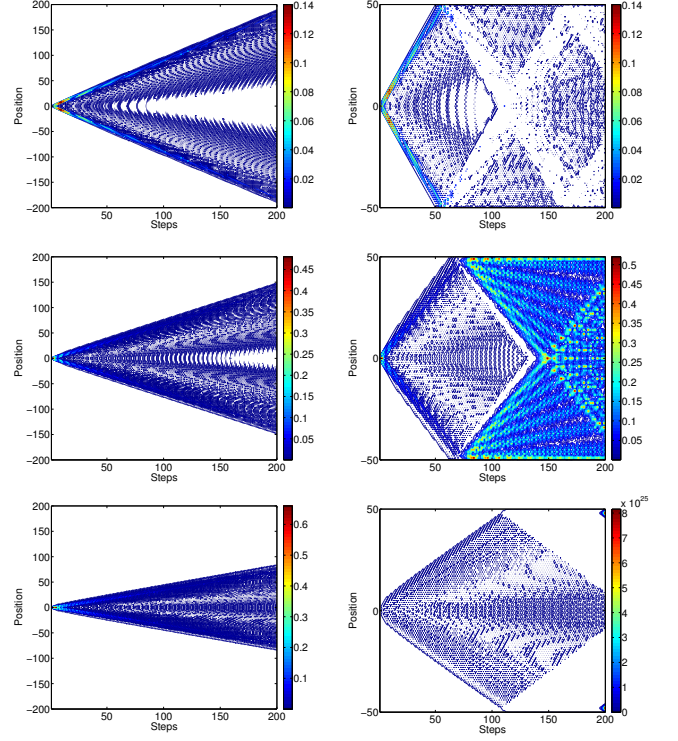


FIG. 4. Density plot of the degree of interference μ for bounded and unbounded DTQW as a function of the time steps and the position. Panels (a) and (b) describe the behaviour of μ for $\theta = \pi/8$, left panel for unbounded and right panel for bounded DTQW, respectively. Similarly, (c) and (d) corresponds to the dynamics for $\theta = \pi/4$ and (e) and (f) corresponds to $\theta = 3\pi/8$. The bounded walker is moving in the interval $[-50, 50]$. The initial state of the walker is $|+\rangle \otimes |x=0\rangle$.

is apparent from the plot, we have that after an initial transient, the ratio saturates to a constant value. More explicitly, it means that performing measurements involving the sole position degree of freedom of DTQW provides a considerable information about the coin parameter (quantified by $H_w(\theta)$), when compared to the full information that it is in principle available (quantified by $H_f(\theta)$). Notice that by measurements performed on the position degree of freedom we *do not mean* just position measurement (whose performances are investigated in the next Subsection) but rather *any* possible measurement on the walker's position Hilbert space.

Fig. 6 shows the walker QFI $H_w(\theta)$ as a function of θ , for different, fixed, numbers of time steps for both unbounded and bounded DTQW. It shows that $H_w(\theta)$ increases with θ initially and then slowly decreases upto $\theta = \pi/2$. For θ ranging from $\theta = \pi/2$ to $\theta = \pi$ the behaviour is mirrored, because of the symmetry of the quantum coin operation between. As it may be seen from the plots the behaviour of the QFIs for unbounded and bounded DTQW are very similar, except from few more

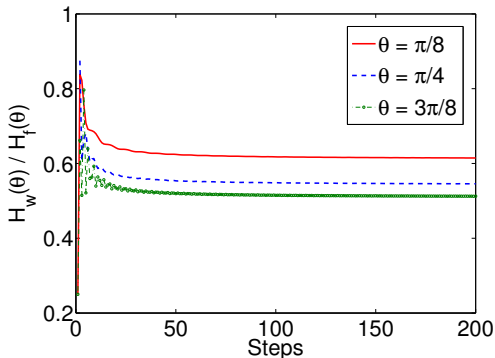


FIG. 5. Ratio of quantum Fisher information in position Hilbert space \mathcal{H}_p to quantum Fisher information in complete Hilbert space $\mathcal{H} = \mathcal{H}_c \otimes \mathcal{H}_p$ for unbounded discrete-time quantum walk for 200-time step and different value of θ . The initial state of the walker is $|+\rangle \otimes |x = 0\rangle$.

oscillations seen in the bounded case. In other words, the boundless DTQW is not particularly detrimental for its use as a probe for the coin parameter.

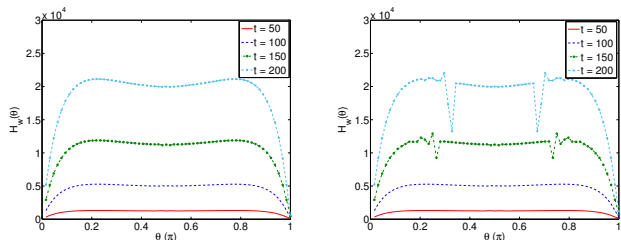


FIG. 6. The walker's position space QFI $H_w(\theta)$ as a function of θ evaluated after a different number of time-steps. The differences between the QFI $H_w(\theta)$ of unbounded and bounded DTQW is again due to interference effects in bounded DTQW. The initial state of the walker is $|+\rangle \otimes |x = 0\rangle$.

C. The FI of walker's position measurement in discrete-time quantum walk

We now turn attention to the performances of specific measurement, perhaps the most natural one may think about, i.e. the measurement on the position of the walker. The conditional probability of finding the walker at position x at time t , given that the value of the coin parameter is θ , is given by $p(x|\theta) = \text{Tr}[\Pi_x \rho_w(\theta)]$ where $\{\Pi_x\} = \{|x\rangle\langle x|\}$ is set of position projection operators, and $\rho_w(\theta)$ is the density matrix of the walker, i.e. the statistical operator of Eq. (17). In other words, the position distribution of the walker is given by the diagonal elements of the density matrix $\rho_w(\theta)$ in the position representation.

Since $\rho_w(\theta)$ is carrying information on θ at any time, measuring the position provides information about the

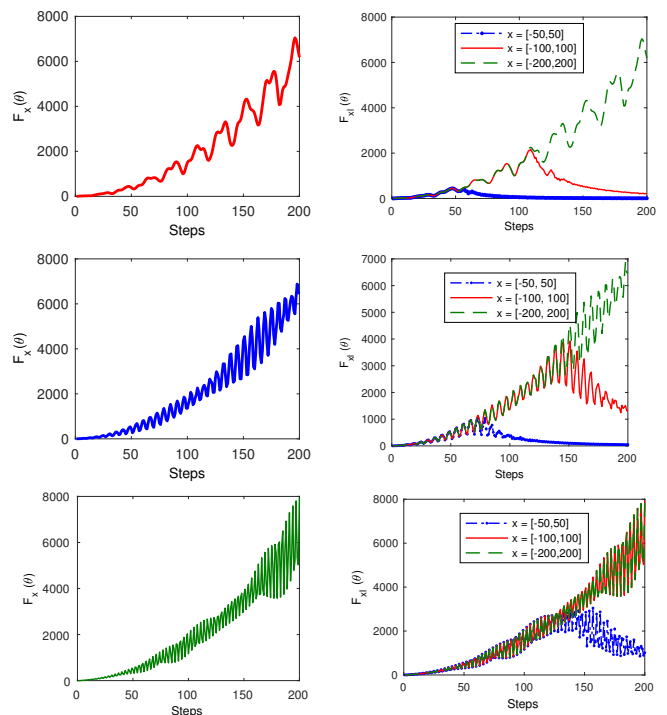


FIG. 7. The Fisher informations $F_x(\theta)$ (left panels) and $F_{x|l}(\theta)$ (right panels) as a function of time for unbounded DTQW and different values of θ . The initial state of the walker is $|+\rangle \otimes |x = 0\rangle$. Both sets of plots are for unbounded DTQW with $F_x(\theta)$ referring to the information extractable by a full position measurement, whereas $F_{x|l}(\theta)$ quantifies the information that may be gained by measurements with limited access to the position of the walker (see text for details). The insets of the right panels are legends for the region S , accessible by the measurement.

value of θ . In order to quantify this information, i.e. to quantify how much information about θ may be obtained by looking at the walker's probability distribution, one has to evaluate the position Fisher information using Eq. (8), i.e.

$$F_x(\theta) = \sum_x \frac{[\partial_\theta p(x|\theta)]^2}{p(x|\theta)}. \quad (24)$$

According to the quantum Cramer-Rao bound we have $F_x(\theta) \leq H_w(\theta)$ and thus, besides the absolute value of $F_x(\theta)$, we are interested in investigating how far is $F_x(\theta)$ from its bound $H_w(\theta)$, i.e. we want to compare the information extracted from position measurement to the maximum information available measuring the sole walker.

The behaviour of $F_x(\theta)$ as a function of time is illustrated in the left panels of Fig. 7 for different values of θ . The FI $F_x(\theta)$ oscillates in time, with the envelope increasing as t^2 , i.e. $F_x(\theta)$ shows the same scaling as $H_w(\theta)$ and $H_f(\theta)$. The right panels illustrate instead the behaviour of the $F_{x|l}(\theta)$, which is the Fisher information of *limited* position measurement, i.e. measurement performed with detectors not able to access (i.e. to *look at*)

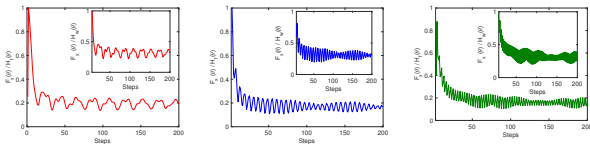


FIG. 8. The ratio $F_x(\theta)/H_f(\theta)$ between the position Fisher information and the full quantum Fisher information as a function of time and for different values of θ . The insets show the ratio $F_x(\theta)/H_w(\theta)$ between the position Fisher information and the walker's position space quantum Fisher information. All the plots refer to unbounded DTQW. The initial state of the walker is $|+\rangle \otimes |x=0\rangle$.

all the possible walker's site, but rather only to a subset S , even though the DTQW is defined on an unbounded position space. According to Eq. (8) we have

$$F_{xl}(\theta) = \sum_{x \in S} \frac{[\partial_\theta p(x|\theta)]^2}{p(x|\theta)}, \quad (25)$$

where the position distribution is still given by $p(x|\theta) = \text{Tr}[\Pi_x \rho_w(\theta)]$, however with $x \in S$. In the right panels Fig. 7 we show the behaviour of $F_{xl}(\theta)$ as a function of time for different values of θ and S . The overall message is that for short time, when the walker has negligible amplitude to be outside S , there are little differences between $F_x(\theta)$ and $F_{xl}(\theta)$, whereas for a number of time steps of the order of $|S|$ the walker is *walking beyond* S and striking differences start to appear. In particular, since in this case the measurement is not recording the full position information, the FI $F_{xl}(\theta)$ starts to decrease with time.

In order to assess the overall performances of position measurements we consider the two ratios $F_x(\theta)/H_f(\theta)$ and $F_x(\theta)/H_w(\theta)$ between the Fisher information of position measurement and the full QFI or the walker QFI respectively. In Fig. 8 we show both the ratios as function of time and for different values of the coin parameter θ .

IV. CONCLUSION

In this paper, we have investigated probing techniques for the coin parameter θ of DTQW which, in turn, plays

a crucial role in providing quadratic speed-up over its classical counterpart. In particular, we have addressed the ultimate bounds to precision, as obtained by performing the optimal measurement on the particle. Our approach is based on the fact that the walker's coin space entangles with the position space after the very first step of the evolution, such that we may estimate the value of the coin parameter θ by performing measurements on the sole position space of the walker.

We have found that the quantum Fisher information (QFI) of the walker's position space $H_w(\theta)$ increases with θ and with time which, in turn, may be seen as a metrological resource. We also find a difference in the QFI of *bounded* and *unbounded* DTQWs, and provide an interpretation of the different behaviours in terms of interference in the position space. We have also compared $H_w(\theta)$ to the full QFI $H_f(\theta)$, i.e. the QFI of the walker's position + coin state, and find that their ratio is dependent on θ , but saturates to a constant value, meaning that the walker may probe its coin parameter quite faithfully. Finally, we have found that if one has access to a limited region in position space, the QFI depends only on the sites with non-zero probability of finding particle. Therefore, when one has access to an incomplete position space, after some steps (which is equal to half of the number of accessible sites) we see a decrease of QFI.

Our results show that estimation of the coin parameter DTQW is possible with realistic detection schemes, and pave the way for further developments in the field of quantum probing for complex networks.

ACKNOWLEDGMENT

CMC would like to thank Department of Science and Technology, Government of India for the Ramanujan Fellowship grant No.:SB/S2/RJN-192/2014. This work has been supported by SERB through project VJR/2017/000011. MGAP is member of GNFM-INdAM.

-
- [1] G. V. Ryazanov, "The feynman path integral for the dirac equation," *JETP*, vol. 6, no. 6, pp. 1107–1113, 1958.
 - [2] R. P. Feynman, "Quantum mechanical computers," *Foundations of physics*, vol. 16, no. 6, pp. 507–531, 1986.
 - [3] K. R. Parthasarathy, "The passage from random walk to diffusion in quantum probability," *Journal of Applied Probability*, vol. 25, pp. 151–166, 1988.
 - [4] Y. Aharonov, L. Davidovich, and N. Zagury, "Quantum random walks," *Physical Review A*, vol. 48, no. 2, p. 1687, 1993.
 - [5] D. A. Meyer, "From quantum cellular automata to quantum lattice gases," *Journal of Statistical Physics*, vol. 85, no. 5-6, pp. 551–574, 1996.
 - [6] J. Kempe, "Quantum random walks: an introductory overview," *Contemporary Physics*, vol. 44, no. 4, pp. 307–327, 2003.
 - [7] S. E. Venegas-Andraca, "Quantum walks: a comprehensive review," *Quantum Information Processing*, vol. 11, p. 1079, 2012.

- no. 5, pp. 1015–1106, 2012.
- [8] A. M. Childs, R. Cleve, E. Deotto, E. Farhi, S. Gutmann, and D. A. Spielman, “Exponential algorithmic speedup by a quantum walk,” in *Proceedings of the thirty-fifth annual ACM symposium on Theory of computing*, pp. 59–68, ACM, 2003.
 - [9] A. M. Childs and J. Goldstone, “Spatial search by quantum walk,” *Physical Review A*, vol. 70, no. 2, p. 022314, 2004.
 - [10] A. Ambainis, “Quantum walk algorithm for element distinctness,” *SIAM Journal on Computing*, vol. 37, no. 1, pp. 210–239, 2007.
 - [11] F. Magniez, M. Santha, and M. Szegedy, “Quantum algorithms for the triangle problem,” *SIAM Journal on Computing*, vol. 37, no. 2, pp. 413–424, 2007.
 - [12] H. Buhrman and R. Špalek, “Quantum verification of matrix products,” in *Proceedings of the seventeenth annual ACM-SIAM symposium on Discrete algorithm*, pp. 880–889, Society for Industrial and Applied Mathematics, 2006.
 - [13] E. Farhi, J. Goldstone, and S. Gutmann, “A quantum algorithm for the hamiltonian nand tree,” *arXiv preprint quant-ph/0702144*, 2007.
 - [14] N. Konno, “Quantum walks,” in *Quantum potential theory*, pp. 309–452, Springer, 2008.
 - [15] G. S. Engel, T. R. Calhoun, E. L. Read, T.-K. Ahn, T. Mančal, Y.-C. Cheng, R. E. Blankenship, and G. R. Fleming, “Evidence for wavelike energy transfer through quantum coherence in photosynthetic systems,” *Nature*, vol. 446, no. 7137, p. 782, 2007.
 - [16] M. Mohseni, P. Rebentrost, S. Lloyd, and A. Aspuru-Guzik, “Environment-assisted quantum walks in photosynthetic energy transfer,” *The Journal of chemical physics*, vol. 129, no. 17, p. 11B603, 2008.
 - [17] C. Chandrashekar and T. Busch, “Quantum percolation and transition point of a directed discrete-time quantum walk,” *Scientific reports*, vol. 4, p. 6583, 2014.
 - [18] B. Kollár, T. Kiss, J. Novotný, and I. Jex, “Asymptotic dynamics of coined quantum walks on percolation graphs,” *Physical review letters*, vol. 108, no. 23, p. 230505, 2012.
 - [19] B. L. Douglas and J. B. Wang, “A classical approach to the graph isomorphism problem using quantum walks,” *Journal of Physics A: Mathematical and Theoretical*, vol. 41, no. 7, p. 075303, 2008.
 - [20] A. M. Childs, “Universal computation by quantum walk,” *Physical review letters*, vol. 102, no. 18, p. 180501, 2009.
 - [21] A. Joye, “Dynamical localization for d-dimensional random quantum walks,” *Quantum Information Processing*, vol. 11, no. 5, pp. 1251–1269, 2012.
 - [22] C. Chandrashekar, “Disorder induced localization and enhancement of entanglement in one-and two-dimensional quantum walks,” *arXiv preprint arXiv:1212.5984*, 2012.
 - [23] C. Chandrashekar and T. Busch, “Localized quantum walks as secured quantum memory,” *EPL (Europhysics Letters)*, vol. 110, no. 1, p. 10005, 2015.
 - [24] H. Obuse and N. Kawakami, “Topological phases and delocalization of quantum walks in random environments,” *Physical Review B*, vol. 84, no. 19, p. 195139, 2011.
 - [25] T. Kitagawa, M. S. Rudner, E. Berg, and E. Demler, “Exploring topological phases with quantum walks,” *Physical Review A*, vol. 82, no. 3, p. 033429, 2010.
 - [26] A. Mallick, S. Mandal, and C. Chandrashekar, “Neutrino oscillations in discrete-time quantum walk framework,” *The European Physical Journal C*, vol. 77, no. 2, p. 85, 2017.
 - [27] G. Di Molfetta and A. Pérez, “Quantum walks as simulators of neutrino oscillations in a vacuum and matter,” *New Journal of Physics*, vol. 18, no. 10, p. 103038, 2016.
 - [28] F. W. Strauch, “Relativistic quantum walks,” *Physical Review A*, vol. 73, no. 5, p. 054302, 2006.
 - [29] C. Chandrashekar, S. Banerjee, and R. Srikanth, “Relationship between quantum walks and relativistic quantum mechanics,” *Physical Review A*, vol. 81, no. 6, p. 062340, 2010.
 - [30] C. Chandrashekar, “Two-component dirac-like hamiltonian for generating quantum walk on one-, two-and three-dimensional lattices,” *Scientific reports*, vol. 3, p. 2829, 2013.
 - [31] G. Di Molfetta, M. Brachet, and F. Debbasch, “Quantum walks as massless dirac fermions in curved space-time,” *Physical Review A*, vol. 88, no. 4, p. 042301, 2013.
 - [32] G. Di Molfetta, M. Brachet, and F. Debbasch, “Quantum walks in artificial electric and gravitational fields,” *Physica A: Statistical Mechanics and its Applications*, vol. 397, pp. 157–168, 2014.
 - [33] P. Arrighi, S. Facchini, and M. Forets, “Quantum walking in curved spacetime,” *Quantum Information Processing*, vol. 15, no. 8, pp. 3467–3486, 2016.
 - [34] A. Pérez, “Asymptotic properties of the dirac quantum cellular automaton,” *Physical Review A*, vol. 93, no. 1, p. 012328, 2016.
 - [35] C. A. Ryan, M. Laforest, J.-C. Boileau, and R. Laflamme, “Experimental implementation of a discrete-time quantum random walk on an nmr quantum-information processor,” *Physical Review A*, vol. 72, no. 6, p. 062317, 2005.
 - [36] A. Schreiber, K. N. Cassemiro, V. Potoček, A. Gábris, P. J. Mosley, E. Andersson, I. Jex, and C. Silberhorn, “Photons walking the line: a quantum walk with adjustable coin operations,” *Physical review letters*, vol. 104, no. 5, p. 050502, 2010.
 - [37] M. A. Broome, A. Fedrizzi, B. P. Lanyon, I. Kassal, A. Aspuru-Guzik, and A. G. White, “Discrete single-photon quantum walks with tunable decoherence,” *Physical Review Letters*, vol. 104, no. 15, p. 153602, 2010.
 - [38] A. Peruzzo, M. Lobino, J. C. Matthews, N. Matsuda, A. Politi, K. Poulios, X.-Q. Zhou, Y. Lahini, N. Ismail, K. Wörhoff, *et al.*, “Quantum walks of correlated photons,” *Science*, vol. 329, no. 5998, pp. 1500–1503, 2010.
 - [39] H. B. Perets, Y. Lahini, F. Pozzi, M. Sorel, R. Morandotti, and Y. Silberberg, “Realization of quantum walks with negligible decoherence in waveguide lattices,” *Physical review letters*, vol. 100, no. 17, p. 170506, 2008.
 - [40] M. Karski, L. Förster, J.-M. Choi, A. Steffen, W. Alt, D. Meschede, and A. Widera, “Quantum walk in position space with single optically trapped atoms,” *Science*, vol. 325, no. 5937, pp. 174–177, 2009.
 - [41] H. Schmitz, R. Matjeschk, C. Schneider, J. Glueckert, M. Enderlein, T. Huber, and T. Schaetz, “Quantum walk of a trapped ion in phase space,” *Physical review letters*, vol. 103, no. 9, p. 090504, 2009.
 - [42] F. Zähringer, G. Kirchmair, R. Gerritsma, E. Solano, R. Blatt, and C. Roos, “Realization of a quantum walk with one and two trapped ions,” *Physical review letters*, vol. 104, no. 10, p. 100503, 2010.

- [43] C. Chandrashekar, R. Srikanth, and R. Laflamme, “Optimizing the discrete time quantum walk using a su (2) coin,” *Physical Review A*, vol. 77, no. 3, p. 032326, 2008.
- [44] A. Smirne, S. Cialdi, G. Anelli, M. G. Paris, and B. Vaccini, “Quantum probes to experimentally assess correlations in a composite system,” *Physical Review A*, vol. 88, no. 1, p. 012108, 2013.
- [45] C. Benedetti, F. Buscemi, P. Bordone, and M. G. Paris, “Quantum probes for the spectral properties of a classical environment,” *Physical Review A*, vol. 89, no. 3, p. 032114, 2014.
- [46] M. G. Paris, “Quantum probes for fractional gaussian processes,” *Physica A: Statistical Mechanics and its Applications*, vol. 413, pp. 256–265, 2014.
- [47] C. Benedetti and M. G. Paris, “Characterization of classical gaussian processes using quantum probes,” *Physics Letters A*, vol. 378, no. 34, pp. 2495–2500, 2014.
- [48] M. A. Rossi and M. G. Paris, “Entangled quantum probes for dynamical environmental noise,” *Physical Review A*, vol. 92, no. 1, p. 010302, 2015.
- [49] D. Tamascelli, C. Benedetti, S. Olivares, and M. G. Paris, “Characterization of qubit chains by feynman probes,” *Physical Review A*, vol. 94, no. 4, p. 042129, 2016.
- [50] L. Seveso and M. G. Paris, “Can quantum probes satisfy the weak equivalence principle?,” *Annals of Physics*, vol. 380, pp. 213–223, 2017.
- [51] M. Bina, F. Grasselli, and M. G. Paris, “Continuous-variable quantum probes for structured environments,” *Physical Review A*, vol. 97, no. 1, p. 012125, 2018.
- [52] C. Benedetti, F. S. Sehdaran, M. H. Zandi, and M. G. Paris, “Quantum probes for the cutoff frequency of ohmic environments,” *Physical Review A*, vol. 97, no. 1, p. 012126, 2018.
- [53] F. Troiani and M. G. Paris, “Universal quantum magnetometry with spin states at equilibrium,” *Physical review letters*, vol. 120, no. 26, p. 260503, 2018.
- [54] A. Beggi, L. Razzoli, P. Bordone, and M. G. Paris, “Probing the sign of the hubbard interaction by two-particle quantum walks,” *Physical Review A*, vol. 97, no. 1, p. 013610, 2018.
- [55] I. Pizio, S. Singh, C. Chandrashekar, and M. G. Paris, “Quantum probes for quantum wells,” *arXiv preprint arXiv:1808.06757*, 2018.
- [56] M. G. Paris, “Quantum estimation for quantum technology,” *International Journal of Quantum Information*, vol. 7, no. supp01, pp. 125–137, 2009.
- [57] S. Singh and C. Chandrashekar, “Interference in localized quantum walk,” *arXiv preprint arXiv:1711.06217*, 2017.
- [58] M. Štefaňák, I. Jex, and T. Kiss, “Recurrence and pólya number of quantum walks,” *Physical review letters*, vol. 100, no. 2, p. 020501, 2008.
- [59] C. Chandrashekar, “Fractional recurrence in discrete-time quantum walk,” *Open Physics*, vol. 8, no. 6, pp. 979–988, 2010.